Hα SURGES AND ASSOCIATED SOFT X-RAY LOOPS

B. SCHMIEDER
Observatoire de Paris, Section de Meudon, DASOP, F-92195 Meudon Principal Cedex, France
K. SHIBATA
National Astronomical Observatory, Mitaka, Tokyo 181, Japan
L. VAN DRIEL-GESZTELYI
Kiso Observatory, The University of Tokyo, Mitake, Kiso, Nagano 397 – 01, Japan
and
S. FREELAND
Lockheed Palo Alto Research Laboratory, Palo Alto, CA 94304, USA.

(Received 3 June, 1994; in revised form 16 September, 1994)

Abstract. A recurrent Hα surge was observed on 7 October, 1991 on the western solar limb with the Meudon MSDP spectrograph. The GOES satellite recorded X-ray subflares coincident with all three events. During two of the surges high-resolution *Yohkoh* Soft X-ray Telescope (SXT) images have been taken. Low X-ray loops overlying the active region where the surges occurred were continuously restructuring. A flare loop appeared at the onset of each surge event and somewhat separated from the footpoint of the surge. The loops are interpreted as causally related to the surges. It is suggested that surges are due to magnetic reconnection between a twisted cool loop and open field lines. Cold plasma bubbles or jets squeezed among untwisting magnetic field lines could correspond to the surge material. No detection was made of either X-ray emission along the path of the surges or X-ray jets, possibly because of the finite detection threshold of the *Yohkoh* SXT.

1. Introduction

The term 'surge' has been used historically for cold material observed in Hα, while 'jets' refer to observations in hotter lines (UV and X-ray lines). The association between them is not clear. Rust, Webb, and MacCombie (1977) analysed 54 Hα surges and *Skylab* soft-X-ray images. They did not find X-ray emission co-spatial with the surges, but they showed that many of the surges were near flares. With the HXIS instrument of SMM, Schadee and Martin (1986) found a decreasing relationship between flares/subflares/microflares and X-ray brightenings. Schmieder *et al.* (1988, 1993) and Harrison, Rompolt, and Garzcynska (1988) associated weak X-ray signatures with the bright Hα bright base of surges. Švestka, Fárník, and Tang (1990) observed X-ray emission of short duration (tens of seconds) from surges that are bright in Hα.

Hα surges last about 30 min and are recurrent with a period of one hour or more (Schmieder *et al.*, 1984). Often emerging flux is observed at the base of the surge (Kurokawa and Kawai, 1993), or an isolated (so-called parasitic) polarity is detected in the longitudinal magnetic field maps. Material is ejected along straight lines and a type III burst may be registered (Chiuderi, Mein, and Pick, 1986). Therefore,

Solar Physics **156:** 245–264, 1995.

Schmieder *et al.* (1988) concluded that ejection of material occurs in open field lines tied close to the footpoint of large loops overlying the active region, and the material subsequently descends with a decelerated free fall motion (Schmieder *et al.*, 1993). Twisted flux tubes or helical motion are also often observed during this phase (Gu *et al.*, 1994).

Harrison, Rompolt and Garzcynska, (1988) gave two possible interpretations, of the brightening in X-rays, which indicate either the cause or the effect. The X-ray bubble, or a kind of X-ray bright point, could represent a volume which has been suddenly heated, so matter is expelled from its vicinity by the corresponding increase in pressure. Alternatively, the heating at the footpoint might be due to a pressure increase when the material is falling back into the chromosphere.

In order to distinguish between these two interpretations, it is important to know the timing of the events, but this is difficult to achieve since surges are recurrent and each of them consists of several X-ray spikes, corresponding to different branches of the surge. The brightness of the cold plasma is delayed by 3 – 4 min compared to the X-ray and UV brightening (Schmieder, Golub, and Antiochos, 1994). The maximum upward velocity occurs usually 10 to 20 min after the X-ray spike.

Theoretical studies seek to explain the ejection of cool plasma by a gradient pressure mechanism (Steinolfson *et al.*, 1979; Shibata *et al.*, 1982) or by magnetic pressure and tension forces (Shibata *et al.*, 1992). The first mechanism has recently been rejected based on two different arguments. Using coordinated observations between NIXT and MSDP, Schmieder, Golub, and Antiochos (1994) demonstrated that the pressure gradient model is not consistent with the observed weak X-ray signature of surges. Shibata *et al.* (1992) rejected the assumption used for the pressure gradient model of a rigid magnetic flux tube, showing that a multi-dimensional magnetic field structure is needed to obtain a mixture of hot and cold plasma. Instead, they proposed a model based on magnetic reconnection associated with emerging magnetic flux in a pre-existing coronal field. The model starts with a compact flare or an X-ray bright point, creating multiple islands which confine cool, dense chromospheric plasma in a sheet. Such a mechanism has been proposed by Raadu *et al.* (1987) to explain eruptive prominences. These islands coalesce and material is ejected at the Alfvén speed (50 – 100 km s^{-1}), in agreement with the observations (Schmieder *et al.*, 1983; Kurokawa, 1988).

The coronal temperature (T_{cor}) would increase significantly as a result of magnetic reconnection. The maximum temperature is of the order of $1/\beta \times T_{cor}$, where β is the ratio of the gas and magnetic pressure. For $T_{cor} = 3 \times 10^5 - 10^6$ K and β^{-1} of the order of 10, we could expect material of $10^6 - 10^7$ K, so the *Yohkoh* Soft X-ray Telescope (SXT) provides an exellent opportunity to test this model (cf., Section 2.3). In a first analysis of the recently discovered X-ray jets, Shibata, Nozawa, and Matsumoto, (1992) showed Hα observations simultaneous with one of the X-ray jets observed by the SXT on 25 February, 1992. They found a good correspondence between the bright footpoint of an Hα surge and the base of the X-ray jet. Furthermore, they detected X-ray emission nearly co-spatial with the

Hα surge, but the X-ray jet was shorter both in length and duration than the Hα surge.

In this paper we present a study of three events using simultaneous observations of NOAA AR 6850 on 7 October, 1991, made with the MSDP operating on the solar tower in Meudon and with the *Yohkoh* SXT. We analyse Hα and SXT data of a recurrent surge observed close to the western limb in order to find clues for the mechanism of chromospheric ejections. We first present the observational data: describe the magnetic configuration, the timing of the surges, the kinetic energy involved, the thermal conditions, and we conclude with a discussion of a possible theoretical model.

2. Instruments and Data

2.1. MAGNETOGRAMS

Magnetograms of the surging region NOAA AR 6850 are available from Okayama on 9, 10, 11 September and on 2, 3, 7 October, 1991 (Sakurai and Koyano, 1992), from Huairou on 4, 5, 6, 7, October, 1991 (courtesy of Zhang H. Q. and Ai G. X.), and from Mees Observatory, Hawaii on 3, 4, 5, 6 October, 1991 (courtesy of G. Cauzzi). Spectroheliograms from Meudon and the magnetograms available allow us to follow the long-term evolution of the two active regions (Figure 1) (see Section 3.2).

2.2. MSDP SPECTROGRAPH

The Multichannel Subtractive Double Pass (MSDP) instrument used for these observations operates in the Meudon Solar Tower. The MSDP observation periods of this active region are listed below: on 7 October, 1991, 07:40–7:50, 08:45–9:22, 10:20–12:02, 12:03–12:20, 12:29–15:14 UT. The MSDP spectrograph (Mein, 1977) provides 9 different wavelength channels of the same 2-D area of the Sun. Photographic densities are transformed into relative intensities using calibration curves deduced from reference profiles obtained by averaging the observed profiles in quiet solar areas. The observations were obtained in the Hα line with a wavelength step of 0.30 Å. The data allow us to reconstruct, by interpolation, a line profile for each pixel in the field of view. The standard processing method uses the wavelength shift between the centers of the two $\Delta\lambda$ chords ($\pm$ 0.3 Å or 0.6 Å and $\pm$ 0.45 Å or 0.9 Å) in the active profile and in the reference profiles over the field to indicate the Doppler shift, and the relative depth of the chords to determine the relative intensity, ΔI, at each pixel. Thus, maps of intensity fluctuations and Doppler shifts are derived. In Figure 2 maps of the active region ($\sim 3' \times 8'$) corresponding to $\Delta\lambda = 0.6$ Å are displayed, obtained by adding three elementary fields of view ($1' \times 8'$). The spatial resolution of the images is only $\sim 2'$ due to the long exposure time neccessary to observe low emission prominence-like structures. The

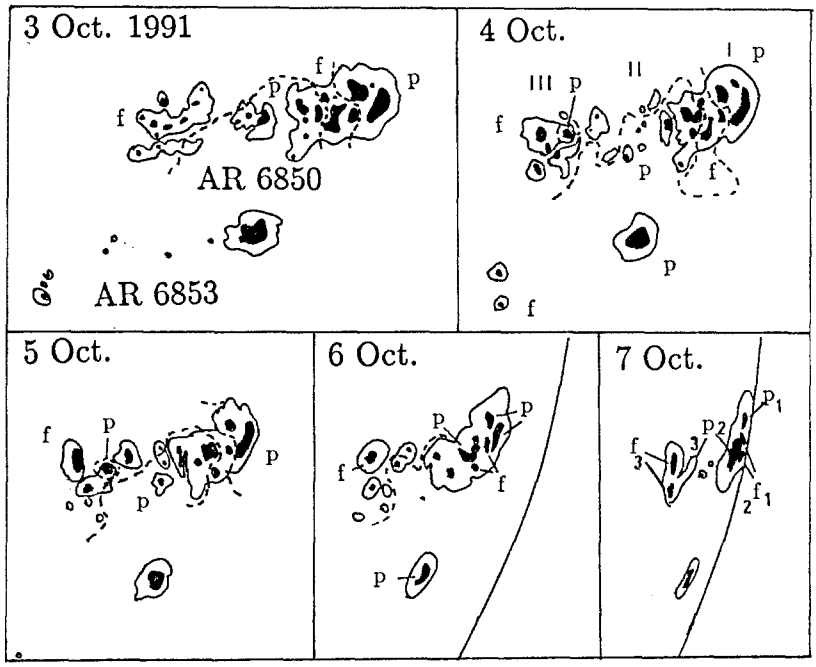

Fig. 1. Spot contours of AR 6850 and 6853 from Meudon spectroheliograms with the magnetic polarity derived from the magnetic maps.

spectral range is limited to 2.4 Å and material with Doppler shifts exceeding 35 to 40 km s^{-1} cannot be seen, even in the extreme channels.

2.3. SXT

On 7 October, 1991 the *Yohkoh* Soft X-ray telescope (SXT) provided several full-disk images per orbit, followed by a set of higher resolution partial frame images (PFI) of 128 × 128 pixels with a pixel size of 2.46″ square. PFIs were obtained successively with the Al.1 (1265 Å) and Al Mg filters, and white-light narrow band images of the same field of view have been taken with the SXT aspect camera (Tsuneta *et al.*, 1991) as well. The thin aluminium (Al.1) and sandwich (Al Mg) filters are most sensitive to temperatures around 3×10^6 K, but can detect X-ray emission as cool as 1.5×10^6 K (Hara *et al.*, 1992). The white-light (Na band) pictures are mainly used for the coalignment (Figure 3). The SXT targeted AR 6850 mainly between 10:02 and 12:15 UT.

3. Observations

The GOES satellite registered subflares on the Sun of class C.2 to C.9 at 08:03, 08:32, 08:42, 10:13, 10:16, and 11:51 UT (Figure 4). The subflare of 10:13 UT

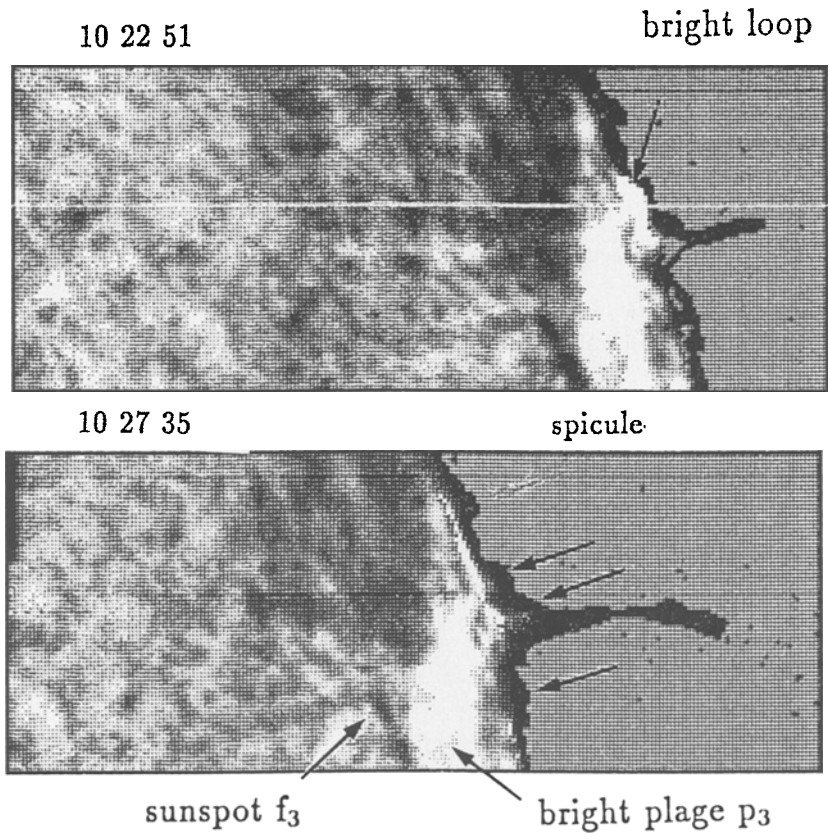

Fig. 2. MSDP observations of the surge in AR 6850 on 7 October, 1991, intensity maps in Hα ± 0.3Å showing a bright loop near the surge, the surge and its triangle base, the sunspot f3, and some spicules indicated by arrows.

occurred in another region, AR 6861 (N08 W24), and the *Yohkoh* satellite shifted to this region for a short time (10:13 – 10:24 UT) thus missing the subflare of 10:16 UT in AR 6850, unfortunately.

3.1. Hα SURGES

In the Hα line a recurrent surge event could be followed in AR 6850, which was especially interesting because of its position close to the limb on 7 October, 1991. In Hα we observed surge activity three times: between 08:46 – 09:11 (spectra have been also obtained in Ondřejov with the Multichannel Flare Spectrograph and will be analysed in a future paper (Kotrč, private communication)), 10:20 – 10:39 and 11:51 – 12:15 UT (Figures 5(a – b) and 6). Note the time-coincidence between the surges and the GOES subflares.

Above this active region we frequently observed spicule-like structures of 10 000 km height. These evolved rapidly, and seemed to be tied in the north-

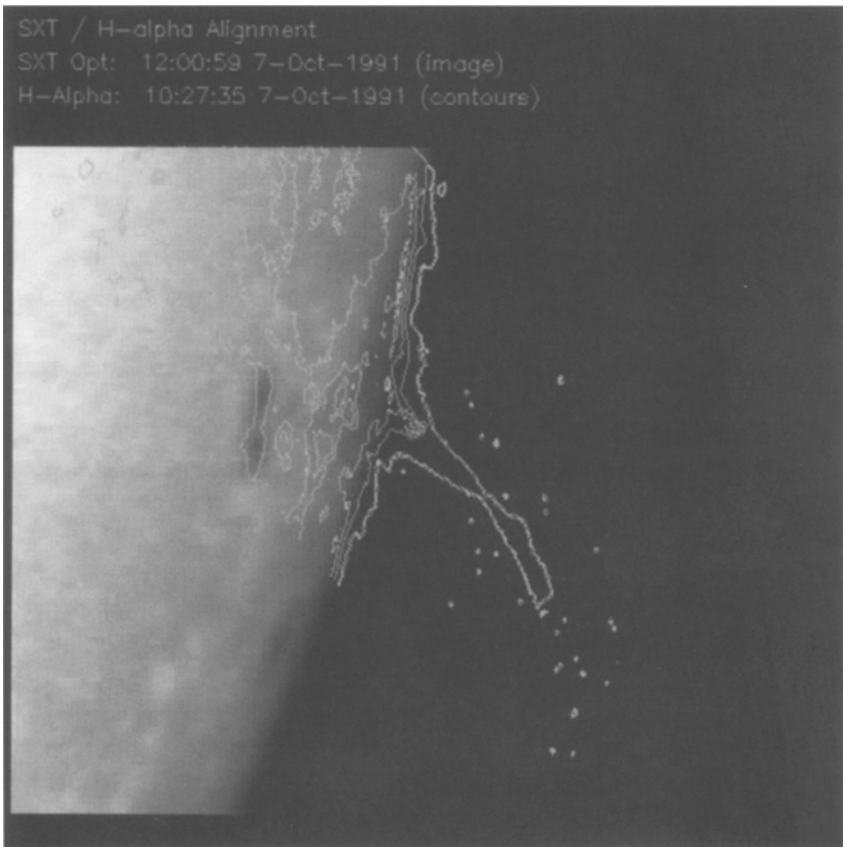

Fig. 3a.

Fig. 3a – c. *Yohkoh* SXT images with MSDP Hα contours superimposed: (a) white-light image (Na band), (b) soft X-ray image obtained with Al.1 filter at 10:27:35 UT, (c) at 12:06 UT.

ern group between the f and p polarity sunspots (f1 f2/p1 p2). Between groups II and III (cf., Figure 1) we observed a large bright plage, corresponding to the polarity (p3) which was related to the site of the flares (Figure 2). In the northern part of this bright plage we observed mainly three spicule-like features (triangle at the base of the surge in Figures 2 and 5(b)), two of them did not produce extensive ejections; they were dense and often loop-shaped. Only the middle one led to a surge. With these low spicule-like features around it, the surge looked like it had multiple footpoints, as suggested by previous observations (e.g., the 'Eiffel tower' of Kurokawa and Kawai, 1993). It is difficult to be sure of the true relationship between these 3 spicule-like features due to the relatively low spatial resolution.

The three observed events had the same development with 3 phases. The first phase was between the occurrence of the X-ray subflare – if we relate all X-ray

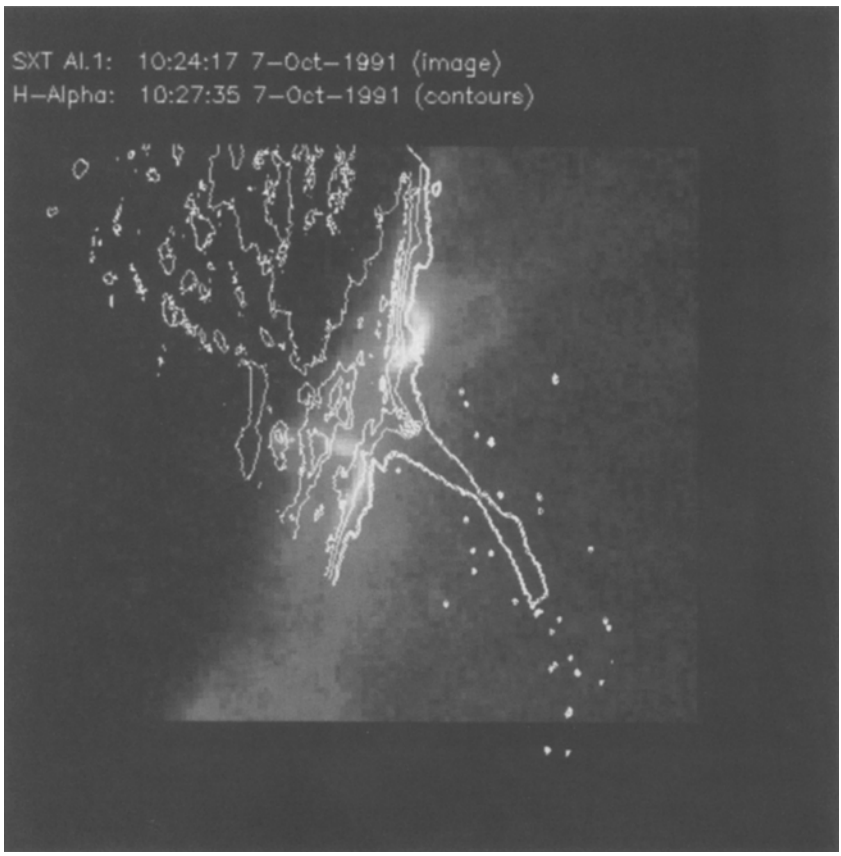

Fig. 3b.

brightenings registered by GOES to the surges – and the beginning of the growing of the spicule-like feature. Corresponding to the appearance of the X-ray subflare we observed an Hα brightness enhancement with a loop shape near the base of the surge to the north of it (Figure 2). This structure may correspond to the so-called flaring arch associated with surges observed by Mouradian, Martres, and Soru-Escaut (1983). During these few ($\sim$ 5) min the spicule-like feature became very dense, as we could see in the third event after 11:51 UT (Figure 5(b)). For the first two events we have missed this phase, however. The Hα observations of the first event began at 08:46 UT, so we missed the 4 min between the beginning of the subflare at 08:42 UT (observed by GOES) and this ejection. The observations of the second surge event began at 10:20:51 UT, when the spicule-like feature was already $\sim$20 000 km long in the red channels. We missed the beginning of the ejection, but from the stage of evolution, e.g., the height of the growing spicules, we can estimate that the event started 4 – 5 min before, corresponding to the time of the subflare registered by GOES at 10:16 UT.

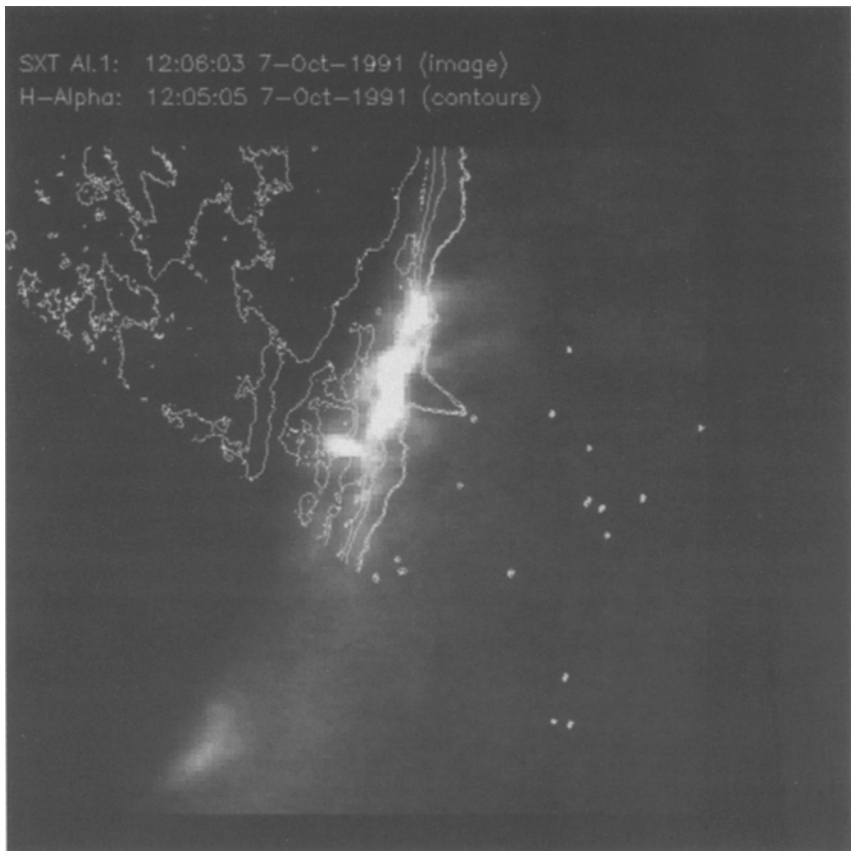

Fig. 3c. .

The second phase lasted for about 10 min, during which the surge was seen mainly in the red channels of the MSDP (Figure 5(a)). Due to perspective effects, material seen in the red channels must be escaping, while material seen in the blue channels must be falling back. The altitude increased, reaching 45 000 km (12:05 UT event) to 75 000 km (10:30 UT event) according to the event considered. The accuracy of the altitude is not better than 5000 km ($\sim$ 10% error).

In the third phase, which lasted for about 10 min, the altitude was decreasing, and at the end the surges were only visible in the last blue channel. The surge was bending during this phase. During the second event at 10:27:05 UT only the footpoint was visible in the blue channels. At 10:28:35 the blueshifted part was extended, and finally at 10:32:20 the entire structure was blueshifted. The matter appeared to go up and down along the same field lines, though it was not a continuous ejection and knots were observed travelling along the lines. From 10:27:05 to 10:35:20 UT the surge material was concentrated in two parts, like two sausages. Faint material was ejected from the top of the surge in two fine threads. It

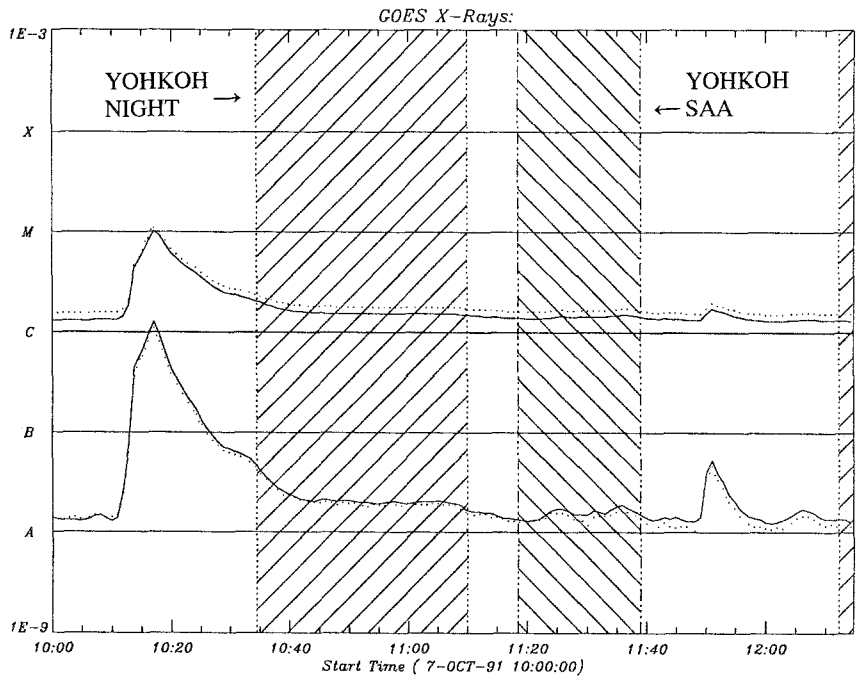

Fig. 4. GOES subflares with the observing periods of *Yohkoh*.

is difficult to see this phenomenon in Figure 5 at 10:35:20 UT, but it is well visible in a video movie made with the images. The surge began to fade at 10:36:50 UT.

3.2. FOOTPOINT OF SURGES

On 7 October, 1991, at the south-western solar limb there were two active regions close to each other: NOAA AR 6850 (S14) and AR 6853 (S30). The northern sunspot group contained at least 3 bipoles (I, II, III in Figure 1), while the southern group was a simple bipole with a dispersed following part. Recurrent surges were observed in the complex region AR 6850. Because of the projection effects it is difficult to define the exact position of the surge events in the sunspot group, but since the overall configuration of the group did not change during its disc passage (Figure 1), there is good reason to believe that the delta configuration persisted on 7 October, when the AR was at the limb and the western part of it was not visible any more. From that and from the overlays (see Figure 1) it looks probable that the flares/surges occurred in delta spot No. I of the northern group (p1 – p2, f1 – f2). A flaring region was observed in front of the large sunspot, f3, of group III and corresponded to one of the footpoints of a small X-ray loop (see Section 3.3).

3.3. SOFT X-RAY LOOPS

Yohkoh pointed at this AR between 10:02 and 10:14 UT, before the MSDP observations of the second event, and after 10:24 UT until the end of the third event at 12:15 UT (Figure 7). Unfortunately the temporal resolution of the sequences is quite poor, since these observations were obtained not long after the satellite started to operate.

In the surging region rapid re-structuring of a complex low-lying loop system was detected. Among these loops a bright point was visible at 10:09 UT which seems to correspond to the base of the surge. Unfortunately it is difficult to be sure of the co-spaciality of these two events due to the perspective effects in the vicinity of the limb. After an observation gap, by 10:24 UT, the loop system appeared to be simplified. Only two loops were visible. The northern loop spatially corresponded to an Hα bright loop (Figure 2). The southern loop connected the edge of spot p2 of group II with an f-polarity area, which corresponded to an Hα bright plage. The surge is located between the 2 loops. Frequently, flaring loops are spatially separated from the surge event, like the surge observed at the periphery of an X-ray emission region with HXIS/SMM (Schmieder *et al.*, 1988). The X-ray system of loops seen around 11:50 UT was more diffuse than in the previous event. A subflare, including a loop and 1 – 2 bright points, was observed at 11:51 UT at the same place as at 10:09 UT, near the base of the Hα ejecta (Figure 7), while neither the southern loop nor the bright point seen during the former surge were present. This suggests that the recurrent surge event was most probably related to the northern flare loop, while it still might be related to the X-ray bright point of 10:09 UT. This repeated appearance of X-ray activity, its timing and its closeness to the base of the Hα surge support the idea that the flaring loops were somehow X-ray signatures of the surges (Figure 7). But no X-ray jet has been observed with the SXT. The surge channel had no spatial counterpart in X-rays (see, e.g., at 10:24:17 UT). The lack of emission could be due to the sensitivity of the SXT instrument (see next section).

4. Quantitative Parameters

4.1. Hα VELOCITIES

In the velocity maps we see both blueshift and redshift along the surge, mainly near the footpoint. This could be due either to rotation of the flux tubes, or to the presence of a second spicule-like structure having an ascending/descending motion not in phase with the main surge (Figure 5). At higher altitudes in the surge blueshifts were observed during the ascending phase (10:23:06 UT). But the Hα line profiles show that the material was in fact seen in the extreme red channel only, and the computed Doppler shifts are therefore not correct for some pixels (Figure 8, point C). In fact, the velocities of these pixels are higher than 35 km s^{-1},

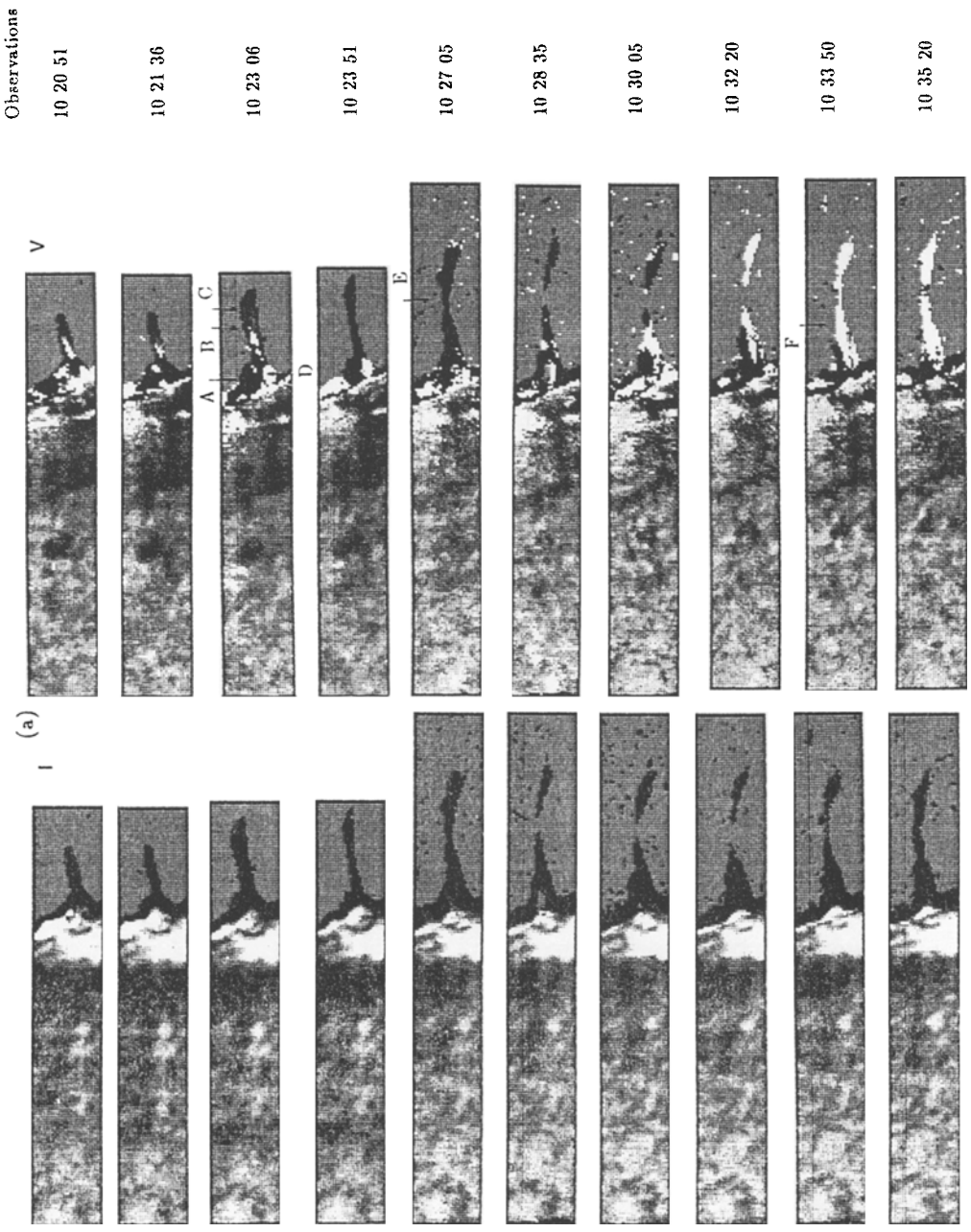
Observations
10 20 51
10 21 36
10 23 06
10 23 51
10 27 05
10 28 35
10 30 05
10 32 20
10 33 50
10 35 20
V
I
(a)
A
B
C
D
E
F

Fig. 5a.

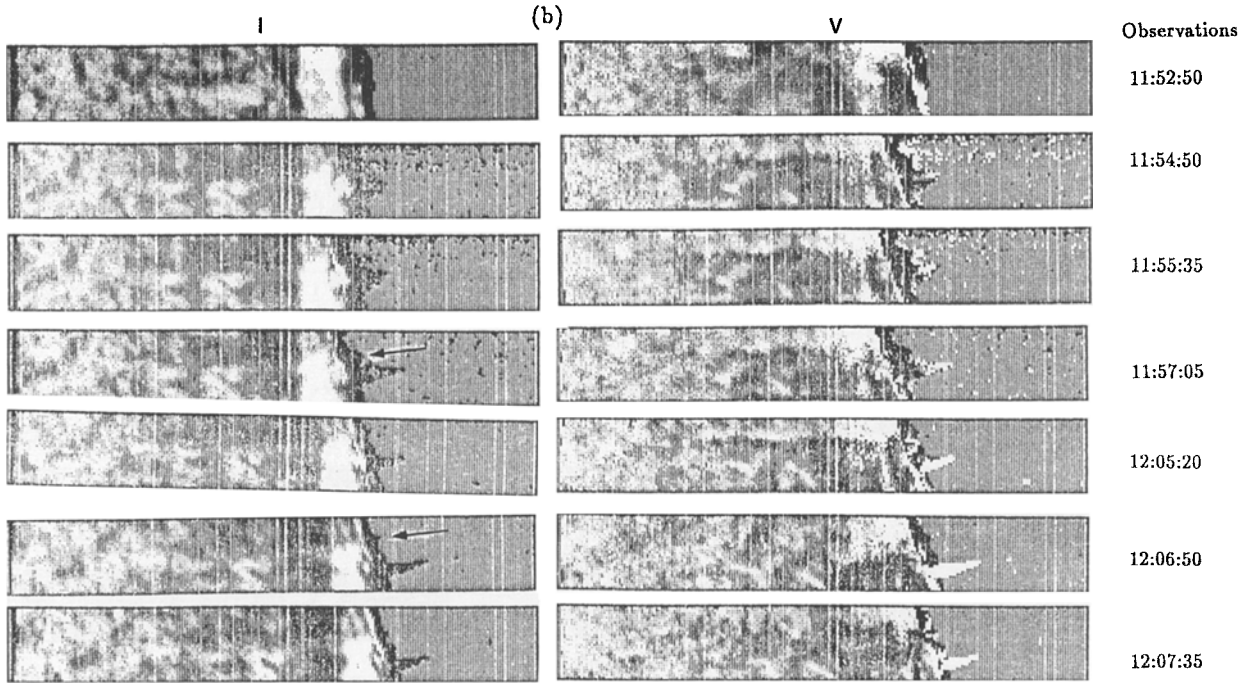

Fig. 5b.

Fig. 5a – b. Time evolution of the surge event (a) around 10:25 UT, (b) around 12:00 UT. The maps, one arc-min wide, were obtained from the MSDP observations in Hα ± 0.3 Å (left pannels: intensity, right pannels: velocity, white/black corresponds to blue/redshift). See Figure 8 for the profiles of the pixels A – F indicated on this figure. Some spicules are indicated by arrows.

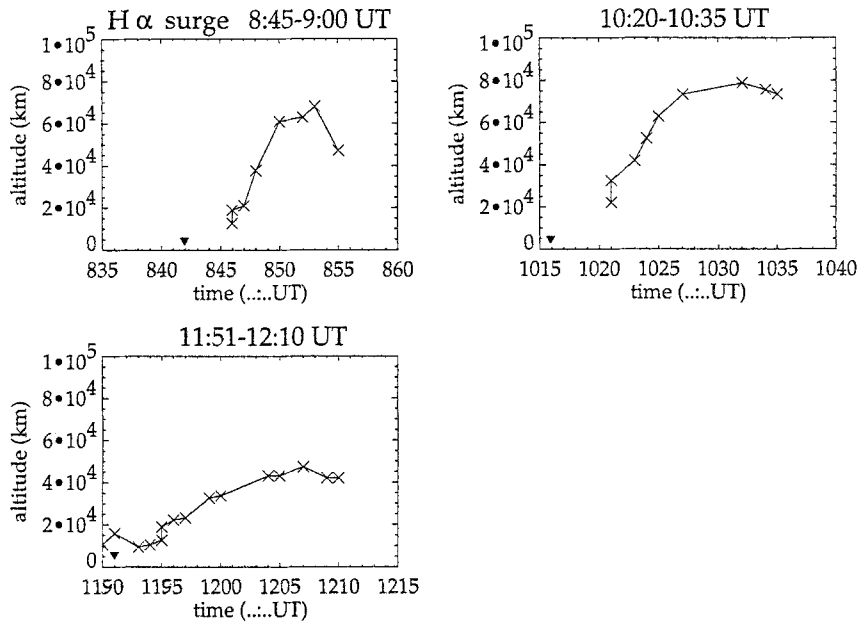

Fig. 6. Curves of the altitudes reached by the tops of the surges; the arrows indicate the occurrence of the X-ray brightenings registered by GOES.

but we can not measure such values (see Section 2.2). The pixels at the top of the surge show high Doppler shifts, consistent with a half-loop shape of the surge in a plane perpendicular to the disk plane and orthogonal to the solar surface.

The velocity component in the image plane, V_r, can be derived from Figure 6. An altitude as high as 75 000 km for the surge of 10:27 UT was reached in 8 min with velocities in the image plane of about 115 km s^{-1}. The maximum altitude of the 12:05 UT event was around 45 000 km, corresponding to a lower velocity ($\sim$ 60 km s^{-1}). The fastest event occurred at 08:45 UT, when a velocity of 200 km s^{-1} was derived.

4.2. KINETIC ENERGY

Doppler shifts of -25 to -30 km s^{-1} are registered as $V_{\pm 0.3\text{Å}}$ and $V_{\pm 0.45\text{Å}}$ in the velocity channels of Hα $\pm$ 0.3 Å and $\pm$0.45 Å at 10:27 UT, and around $+15$ to 20 km s^{-1} at 10:33 UT (Table I and Figure 8). Seen by the inclination (away from us) of the structure (leg of the loop) with respect to the disk plane, the redshifts correspond to upflows and the blueshifts to downflows. Following the top of the surge we have found a velocity, V_r, in the disk plane in the range of 115 km s^{-1} at 10:27:05 UT, indicating an angle, α, for the inclination of the surge towards the disk plane in the range of $\sin\alpha \sim 0.3$ to 0.5 ($\alpha \sim 20°$ to 35°), consistent

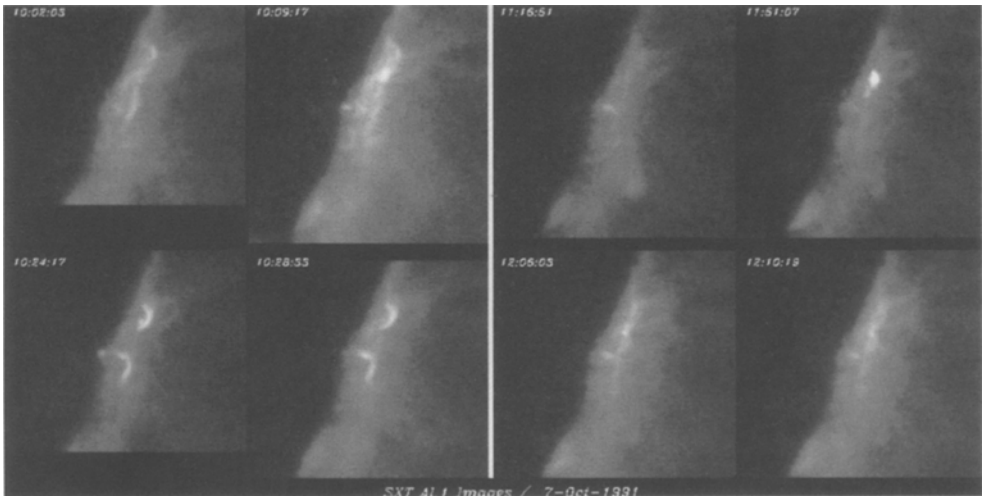

Fig. 7. *Yohkoh* SXT images obtained with the Al.1 filter for the event of 10:25 UT (left panels) and for the event of 12:05 UT (right panels).

with the statistical value (29°) determined for spicules by Heristchi and Mouradian (1992).

The kinetic energy is $E_K = 1/2M(V_r^2 + V_{\pm 0.3\text{Å}}^2)$. For the event of 10:25 UT, E_K is of the order of 10^{28} erg with the mass of the surge material $M = 1.5 \times 10^{14}$ g (see next section). At maximum extent, the potential energy would also be $\sim 10^{28}$ ergs.

4.3. TEMPERATURE AND EMISSION MEASURE

The number of SXT images of the surge between 10:00–10:30 UT is small, only 13 for the thin aluminum filter (Al.1) and 11 for the sandwich filter (Al Mg); there is no image between 10:15 and 10:24 UT. Thus, it is not easy to derive a reliable temperature and emission measure for each pixel, so we examined only the 'average' temperature and emission measure of three regions (the northern flaring loop, surge region, and southern flaring loop), which contained 100–200 pixels each, during 10:00–10:30 UT, using the filter ratio method (Hara *et al.*, 1992). The average value for 100–200 pixels is more reliable since the use of many pixels improves the signal/noise ratio. The results are as follows:

– *Northern loop:* at 10:00–10:05 UT the temperature was $(3-4)\times 10^6$ K and the volume emission measure $= 10^{48}$ cm^{-3}, while at 10:24–10:30 UT the temperature was $(5-6)\times 10^6$ K and the volume emission measure $= (1-2)\times 10^{48}$ cm^{-3}.

The systematic error in the temperature may be of order of $(1-2)\times 10^6$ K. Assuming a loop area of 2×10^{18} cm^2 and a line-of-sight distance of 10^9 cm, the volume of the flaring loop was 2×10^{27} cm^3, implying $n_e = (2-3)\times 10^{10}$ cm^{-3}.

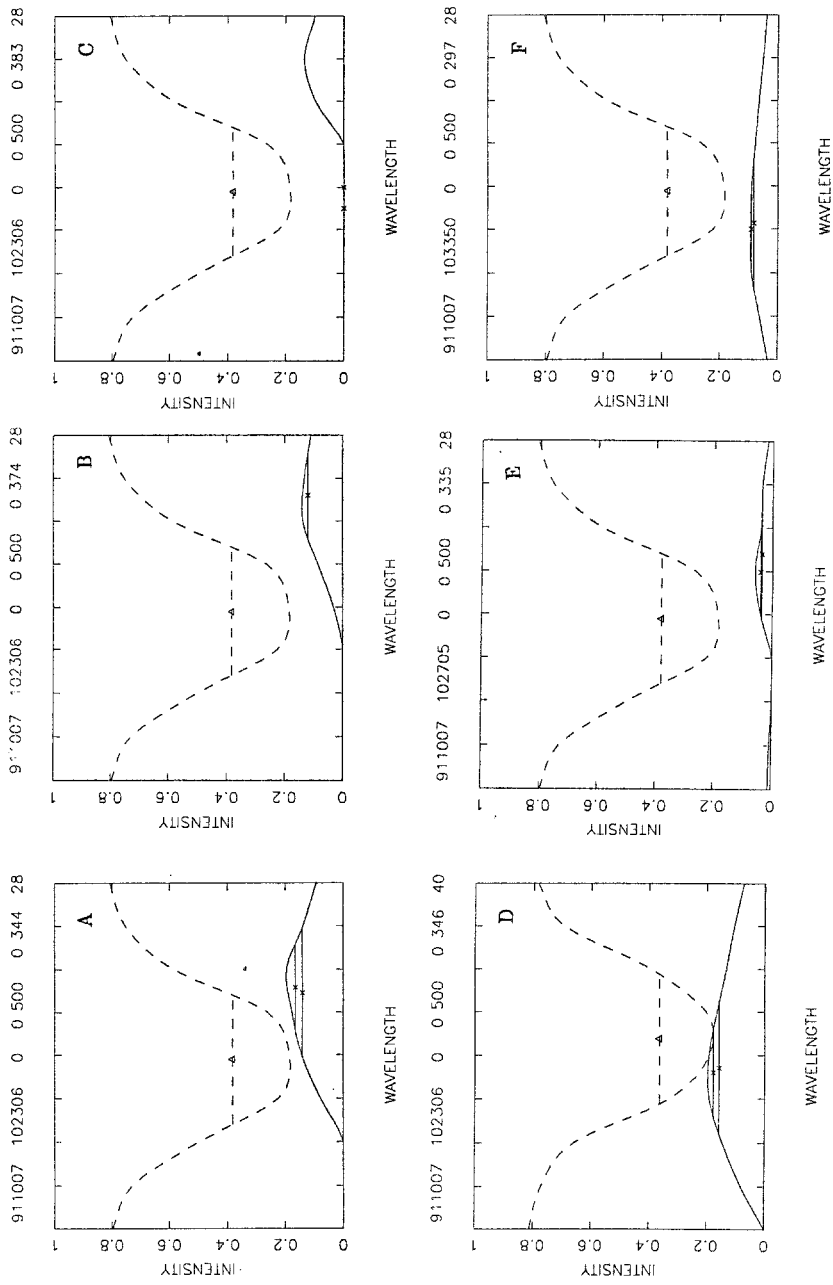

Fig. 8. Hα line profiles for redshifted pixels (A, B, C, E) and for blueshifted pixels (D, F) (cf. Figure 5).

TABLE I
Characteristics of the profiles presented in Figure 8

Point	Time UT	$V_{\pm 0.3Å}$ km s^{-1}	$V_{\pm 0.45Å}$ km s^{-1}	I_{max}/I_c
A	10:23:06	−23	−21.5	0.2
B	10:23:06	−37		0.14
C	10:23:06	>40		0.13
D	10:23:06	10.5	9	0.2
E	10:27:05	−15	−20.7	0.06
F	10:33:50	12	10	0.09

Hence, the total thermal energy content around 10:24 UT was $E_t = 3n_e kTV = (0.8-1.4) \times 10^{29}$ erg, i.e., of order 10^{29} erg.

– *Surge region (mid-part of the surge):* at 10:24 – 10:30 UT the temperature was $(3-4) \times 10^6$ K and the volume emission measure was 10^{47} cm^{-3} Assuming a volume of $(3-10) \times 10^{27}$ cm^3, we derive an electron density $n_e = (3-6) \times 10^9$ cm^{-3}.

Since there was no jet-like feature along the surge, these values refer to the conditions in the corona surrounding the surge. On the other hand, even if an X-ray jet would occur in association with the Hα surge with physical conditions similar to the 12 November, 1991 jet (described in Shibata *et al.*, 1992), which had an average electron density of $(0.4-2) \times 10^9$ cm^{-3}, occurs in association with an Hα surge, it would still be difficult to detect such a faint X-ray jet embedded in bright corona.

Southern loop: at 10:24 – 10:30 UT the temperature was $(4-5) \times 10^6$ K and the volume emission measure = 10^{48} cm^{-3}. Hence, the physical conditions are similar to those of the northern loop.

5. Modelling

We found that the three (recurrent) surge events which were observed in NOAA AR 6850 on 7 October, 1991 between 08:03 and 12:15 UT were coincidental with X-ray subflares as observed by GOES, the X-ray brightening starting about the same time or a few minutes earlier than the growing of the surge. *Yohkoh* SXT observations of the last two surges show the appearance of a flaring loop, and in one case a bright point in the vicinity of the Hα surge event. The X-ray bright point may be related to the footpoint of the surge (although it is not certain), while the X-ray loop, which appeared nearly simultaneously with the surge at both cases at the same place, seemed to be somewhat separated from the footpoint. The presence

of the homologous flare loop coincident with the surge event suggests a causal relationship between these two events.

The association of an X-ray flare with an Hα surge is an important finding, suggesting that surge formation is closely related to energy release occurring in the corona. The relationship between Hα surges and X-ray bright points or jets is still controversial (Shibata *et al.*, 1992; Schmieder, Golub, and Antiochos, 1994). Pressure gradient driven models (Steinolfson, Schmahl, and Wu, 1979) imply some coronal heating, while such heating related to chromospheric ejections was not found in NIXT observations at 63 Å. Schmieder, Golub, and Antiochos (1994) proposed a reconnection model instead. Nevertheless, hot material may be below the detection threshold of the instrument, due to the low electron density of the expected coronal jet plasma, as argued in Section 4.3.

Shibata *et al.* (1992) ruled out all models with a simple pressure driver, for one class of surge associated with X-ray emission, with another argument: if a large amount of energy is injected into the upper chromosphere to create an X-ray emitting plasma, then the cold plasma above the energy injection point is heated up and evolves into X-ray emitting plasma (i.e., it evaporates), so then there is no Hα-emitting cold plasma jet (Sterling *et al.*, 1991; Sterling, Shibata, and Mariska, 1993). That is, an X-ray emitting hot plasma cannot co-exist with a cold plasma within the same rigid flux tube. In order to explain the co-existence of both hot and cold plasma, we have to assume a three-dimensional magnetic field structure (see Yokoyama and Shibata, 1994), where hot and cold plasmas are on different field lines. Heat conduction into the cold plasma would be inhibited by the magnetic field.

In the reconnection model, surge gas is accelerated by the magnetic field as the field releases its stress by exiting the reconnection region. The amount of heating may be small, and it is likely to happen primarily near the reconnection region, low in the chromosphere. Hence, the surge acceleration in the reconnection model could occur without significant coronal heating or X-ray emission. The amount of X-ray emission would depend on temperature and density. For a high-density plasma, like the chromosphere, the temperature may be sufficiently low for only a small amount of X-ray emission to occur. Heating should still occur, however, so if one were to look at lower temperatures, like C IV, stronger emission should be seen there than in X-rays. This is in fact what we have found in previous studies, but a quantitative calculation of the heat associated with this emission has not been made yet. The C IV emission is very strong and sustained (Schmieder *et al.*, 1983), so it really looks like there could be a considerable amount of heat generated at lower temperatures (transition zone temperatures).

Theoretically, X-ray jets could be associated with chromospheric ejections (Shibata, Yokoyama, and Shimojo, 1994). If the reconnection occurs in the transition region or in the upper chromosphere, both hot and cold plasmas could be ejected according to numerical simulations (Shibata, Nozawa, and Matsumoto, 1992; Yokoyama and Shibata, 1993, 1994). If the reconnection occurs in the lower chro-

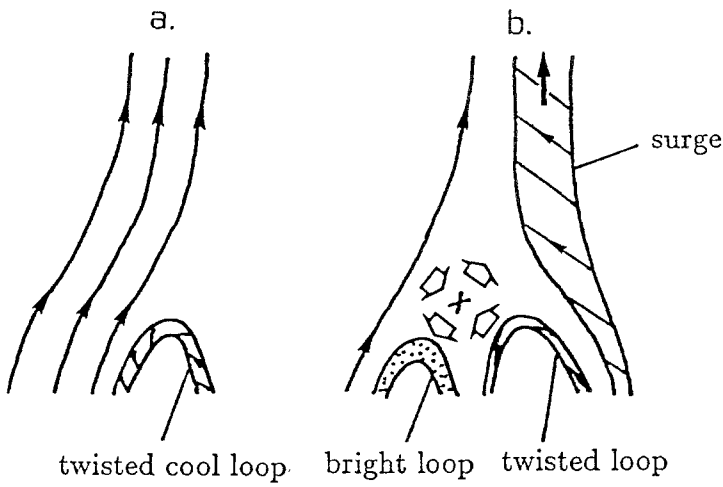

Fig. 9. Schematic illustration of a reconnection between a twisted loop and open field lines leading to an Hα surge and an X-ray flare: (a) original configuration with open field lines and a twisted cool loop, (b) reconnected configuration: hot, X-ray emitting flare loop and cool untwisting surge.

mosphere, we could get only a cool jet, although we need further simulations to confirm this point. On the other hand, if the reconnection point is high in the corona it is not easy to get cool chromospheric ejections by simple reconnection.

Another possibility to get cool jets may be a magnetic twist mechanism (Shibata and Uchida, 1986). Though this mechanism is also closely related to magnetic reconnection, i.e., the magnetic twist stored in cool chromospheric plasma suddenly relaxes and accelerates plasmas as a result of reconnection between twisted and untwisted flux tubes. In this model, reconnection itself could occur in either hot coronal plasma or in cool (upper) chromospheric plasma.

In the case of the surges discussed in this paper, bright X-ray loops appeared nearly simultaneously with the surges at positions somewhat separated from the footpoint of the surges (Figure 9). It should be noted that the simultaneous appearance of surges and X-ray loops could rule out that the jet is accelerated by a nonlinear Alfvén wave, whose origin lies deep inside the atmosphere, propagated along a 'rigid' flux tube (e.g., Hollweg, Jackson, and Galloway, 1982), since such a model cannot explain the appearance of X-ray loops.

The separation of X-ray jets and flare loops has been found in many X-ray jets (Shibata, Yokoyama, and Shimojo, 1994) and could be considered as evidence of magnetic reconnection between a loop and an 'open' field, which produces reconnected loops (bright X-ray loops) and reconnected 'open' fields (surges or jets) at separate locations (see Figure 9). The current sheet at the reconnection region may be too thin to be seen by the SXT and the original loop before the reconnection was too cool to produce a hot jet detectable in X-rays with the SXT.

A similar conclusion has been reached by Rust, Webb and MacCombie, (1977) who used *Skylab* data obtained with a higher detection threshold.

The fact that in our Doppler maps of the Hα surge an untwisting motion of the surge material was apparent, suggests that the cool loop, which would reconnect with the open field lines, was twisted. Then the twist of the cool loop would untwist along the reconnected open field lines surrounding the surge (Shibata and Uchida, 1986). Note that even the changes in the angle of the surge compared to the normal are consistent with the model (cf. Figures 2 and 9): at the beginning the surge was bending towards the reconnected bright X-ray loop, and then it straightened and even curved away from it while the distance between the loop and the surge slightly increased (see also simulations by Yokoyama and Shibata, 1994).

In conclusion, the present study confirms that Hα surges could be explained by a magnetic reconnection model, proposed previously by Shibata *et al.* (1992) and Schmieder, Golub, and Antiochos (1994), following the pioneering idea by Heyvaerts, Priest, and Rust (1977). Future similar surge studies should be based on multiwavelength observations combining optical, X-ray and UV data. The SOHO satellite will provide such information in the future.

Acknowledgements

We are grateful to Drs T. Forbes, S. Antiochos, J. Karpen, and K. Dere for the fruitful discussions that we had with them and to W. van Driel for a critical reading of the paper. B.S. would like to thank to Zhang H. Q. and Ai G. X. for giving her vector magnetograms of the Huairou Observatory during her visit in Huairou and we gratefully thank G. Cauzzi for providing Mees Observatory, University of Hawaii vector magnetograms and Hα pictures. The observations made with the MDSP were performed by C. Coutard and R. Hellier. They were reduced at the MAMA microdensitometer of the Observatory of Paris. One of the authors (BS) wants to thank the *Yohkoh* team during her stay at ISAS (Japan) for helping her in SXT data reduction and B. Bentley for the installation of the *Yohkoh* software at Meudon. Thank is due to an unknown referee for his/her helpful comments, which greatly improved the paper.

References

Chiuderi-Drago, F., Mein, N., and Pick, M.: 1986, *Solar Phys.* **97**, 389.
Gu, X. M., Lin, J., Li, K. J., Xuan, J. Y., Luan, T., and Li, Z. K.: 1994, *Astron. Astrophys.* **282**, 240.
Hara, H., Tsuneta, S., Lemen, J. R., Acton, L. W., and McKiernan, J. M.: 1992, *Publ. Astron. Soc. Japan*, **44**, L135.
Harrison, R.A., Rompolt, B., and Garczynska, I.: 1988, *Solar Phys.* **116**, 61.
Heyvaerts, J., Priest, E. R., and Rust, D. M.: 1977, *Astrophys. J.* 216, 123.
Heristchi, D. and Mouradian, Z.: 1992, *Solar Phys.* **142**, 21.
Hollweg, J., Jackson, S., and Galloway, D. : 1982, *Solar Phys.* **75**, 35.

Kurokawa, H.: 1988, *Vistas Astron.*, **31**, 67.
Kurokawa, H. and Kawai, G.: 1993, *The Magnetic and Velocity Fields of Solar Active Regions*, Astronomical Society of the Pacific Conference Series, **46**, 507.
Mein, P.: 1977, *Solar Phys.* **54**, 45.
Mouradian, Z., Martres, M. J., and Soru-Escaut, I.: 1983, *Solar Phys.* **87**, 309.
Raadu, M.A., Malherbe, J. M., Schmieder, B., and Mein, P.: 1987, *Solar Phys.* **109**, 59.
Rust, D. M., Webb, D. F., and MacCombie, W: 1977, *Solar Phys.* **54**, 53.
Sakurai, T. and Koyano, H.: 1992, *Solar Vector Magnetograms 1991*, Okayama Astrophys. Obs., National Astron. Obs., Japan.
Schadee, A. and Martin, S. F.: 1986, in D. F. Neidig (ed.), *The Lower Atmosphere of Solar Flares*, NSO Publication, 360.
Schmieder, B., Vial, J. C., Mein, P., and Tandberg-Hanssen, E.: 1983, *Astron. Astrophys.* **127**, 337.
Schmieder, B., Malherbe, J. M., Mein, P., and Tandberg-Hanssen, E.: 1984, *Solar Phys.* **94**, 133.
Schmieder, B., Simnett, G. M., Mein, P., and Tandberg-Hanssen, E.: 1988, *Astron. Astrophys.* **201**, 327.
Schmieder, B., van Driel-Gesztelyi, L., Gerlei, O., and Simnett, G. M.: 1993, *Solar Phys.* **146**, 163.
Schmieder, B., Golub, L., and Antiochos, S. K.: 1994 , *Astrophys. J.* 425, 326.
Shibata, K. and Uchida, Y.: 1986, *Solar Phys.* **103**, 299.
Shibata, K., Nozawa, S., and Matsumoto, R.: 1992, *Publ. Astron. Soc. Japan*, **44**, 265.
Shibata, K., Yokoyama, T., and Shimojo, M.: 1994, in S. Enome and T. Hirayama (eds.), *Kofu Meeting Proceedings*, Nobeyama Radio Observatory Report No. 360, p. 75.
Shibata, K., Nishikawa, T., Kitai, R., and Suematsu, Y.: 1982, *Solar Phys.* **77**, 121.
Shibata, K., Ishido, Y., Acton, L. W. *et al.*: 1992, *Publ. Astron. Soc. Japan*, **44**, L173.
Steinolfson, R. S., Schmahl, E. J., and Wu, S. T.: 1979, *Solar Phys.* **63**, 187.
Sterling, A. C., Mariska, J. T., Shibata, K., and Suematsu, Y.: 1991, *Astrophys. J.* 381, 313.
Sterling, A. C., Shibata, K., and Mariska, J. T.: 1993, *Astrophys. J.* 407, 778.
Švestka, Z., Fárník, F., and Tang, F.: 1990, *Solar Phys.* **127**, 149.
Tsuneta, S., Acton, L. W. *et al.*: 1991, *Solar Phys.* **136**, 37.
Yokoyama, T. and Shibata, K.: 1993, ESA SP **351**, 203.
Yokoyama, T. and Shibata, K.: 1994, in S. Enome and T. Hirayama (eds.), *Kofu Meeting Proceedings*, Nobeyama Radio Observatory Report No. 360, p. 367.